International Journal of Nanoelectronics and Materials
*Volume 12, No. 1, Jan 2019* [37-46]

# Preparation and Characterization of Magnetite ($Fe_3O_4$) nanoparticles By Sol-Gel Method

Zakiyyu I. Takai[1,2], Mohd K. Mustafa[1,2*], Saliza Asman[2] and Khairunnadim A. Sekak[3*]

[1]*Microelectronic and Nanotechnology-Shemsuddin Research Centre (Mint-SRC) Uvniversiti Tun Hussein Onn Malaysia (UTHM).*
[2]*Department of Physics and Chemistry, Faculty of Applied Sciences and Technology, Universiti Tun Hussein Onn Malaysia, Educational Hub Pagoh, 84000, Muar, Johor, Malaysia.*
[3] *Faculty of Applied Sciences, Universiti Teknologi Mara. 40450 Shah Alam, Salangor, Malaysia.*

Received 18 March 2018; Revised 12 July 2018; Accepted 29 July 2018

**ABSTRACT**

*The magnetite ($Fe_3O_4$) nanoparticles were successfully synthesized and annealed under vacuum at different temperature. The $Fe_3O_4$ nanoparticles prepared via sol-gel assisted method and annealed at 200-400ºC were characterized by Fourier Transformation Infrared Spectroscopy (FTIR), X-ray Diffraction spectra (XRD), Field Emission Scanning Electron Microscope (FESEM) and Atomic Force Microscopy (AFM). The XRD result indicate the presence of $Fe_3O_4$ nanoparticles, and the Scherer`s Formula calculated the mean particles size in range of 2-25 nm. The FESEM result shows that the morphologies of the particles annealed at 400ºC are more spherical and partially agglomerated, while the EDS result indicates the presence of $Fe_3O_4$ by showing Fe-O group of elements. AFM analyzed the 3D and roughness of the sample; the $Fe_3O_4$ nanoparticles have a minimum diameter of 79.04 nm, which is in agreement with FESEM result. In many cases, the synthesis of $Fe_3O_4$ nanoparticles using $FeCl_3$ and $FeCl_2$ has not been achieved, according to some literatures, but this research was able to obtained $Fe_3O_4$ nanoparticles base on the characterization results.*

**Keyword:** Sol-Gel Method, Magnetite Nanoparticles, Particles Size, Morphologies, XRD.

## 1. INTRODUCTION

Recently, the magnetite ($Fe_3O_4$) nanoparticles have been explored extensively due to their unlimited physical and chemical properties at the nanoscale [1]. In most of the application of magnetite nanoparticles, uniform shape and size particles are required to be well dispersed in the solvent. The major factors that influence the interest of many researchers are the particles size. However, the shape and size of the $Fe_3O_4$ nanoparticles usually controlled by their synthesis techniques. Therefore, synthesis technique is the most significant method for preparation of certain materials, such as metal oxide powder and ceramic materials [2]. Magnetite nanoparticles synthesized with effective properties such as shape, size and suitable morphologies, will help to achieve a wider range of application [3]. Up to now, the focus have been made on the synthesis of iron oxide particles because it can be crystalline in different polymorphic phases which include hematite ($\alpha$-$Fe_2O_3$), maghemite ($\gamma$-$Fe_2O_3$), and magnetite ($Fe_3O_4$) [4]. Among these inorganic nanoparticles, $Fe_3O_4$ nanoparticles has interesting electric and magnetic properties as well as extensive potential applications in colour imaging, magnetic recording media, soft magnetic materials, ferrofluid, spintronic and biomedical applications such as drugs delivery, cell separation, imaging and therapeutic in vivo technology [3,4].

* Corresponding Author: *zitakai21@gmail.com*

Numerous synthesis method like co-precipitation method [5], hydrothermal method [6], microwave irradiation method [7], ultrasonic method [8] and sol-gel method [9] have been used to synthesize magnetite nanoparticles.

Among all synthesis method, sol-gel techniques has been chosen compared to the remaining traditional synthesis techniques due to its advantageous properties including low cost, high purity, and suitable homogeneity [10]. However, in the quest to produce nanoparticles by sol-gel techniques suitable for product, many parameter need to be optimized to control the reaction condition [11,12]. It was gathered that, increasing the reactivity enhance wider surface area of the nanoparticles obtained by sol-gel techniques [13]. In recent time, the attention have been on the preparation of magnetite nanoparticles in order to overcome certain problem, through different chemical synthesis method, although a lot of research have been published demonstrating the preparation of magnetite ($Fe_3O_4$) nanoparticles using several method for different applications such as drug delivery, magnetic recorder, ferrofluid and sensing application [14, 15]. Furthermore, the $Fe_3O_4$ nanoparticles were prepared by [16, 17] through sol-gel method using chepest materials of ferric nitrite as the precusor. The $Fe_3O_4$ nanoparticles was observed at 250ºC. When the temperature rises to 350ºC, the himatate ($Fe_2O_3$) also appear causing major deffiency that hinder its applications [18-20]. In the research reported by [21-23], sol-gel method were used to synthesized iron oxide and its mixture using ethlylene glycol, $FeCl_3$ and $FeCl_2$, but the magnetite nanoparticles has not been observed.

In this work, the $Fe_3O_4$ nanoparticles were prepared effectivitily through sol-gel techniques and it was annealed under vacuum in different temperature. The major material used in the synthesis of $Fe_3O_4$ nanoparticles are iron (III) chloride ($FeCl_3$), iron (II) chloride ($FeCl_2$) and ethylene glycol ($C_2H_6O$). The $Fe_3O_4$ nanoparticles samples are prepared in the form of S1, S2 and S3 with different annealed temperature of 200ºC, 300ºC and 400ºC respectively. The morphologies of the $Fe_3O_4$ nanoparticles annealed at 400ºC were found to be more spherical and partially agglomerated with continues size distribution.

## 2. EXPERIMENTAL METHOD

### 2.1 Materials

Iron (III) chloride $FeCl_3.6H_2O$, Iron (II) chloride $FeCl_2.4H_2O$ and ethylene glycol ($C_2H_6O$) grade were obtained from SIGMA ALDRICH chemical cooperation. The entire reagents were used without any further purification.

### 2.2 Synthesis of $Fe_3O_4$ Nanoparticles

The synthesis of magnetite nanoparticles is described as follows: 2.35g of Fe (III) and 8.35g of Fe (II) were firstly dissolved in 60 ml of ethylene glycol and vigorously stirred for a period of 3h at 45ºC to form a sol. Subsequently, the sol was heated and maintained at a temperature of 80ºC until dark colour gel was formed. This gel was aged for a period of 72h and later dried at 140ºC for 5h. The obtained xerogel was annealed at a certain temperature ranging from 200-400ºC under vacuum condition. Finally, different size magnetite nanoparticles were successfully obtained. The synthesized $Fe_3O_4$ nanoparticles were washed with a certain amount of acetone and ethanol several times to enhance its magnetic properties. Table 1 tabulates the effect of a change in temperature towards the mean size of magnetic nanoparticles calculated from XRD data using Scherer's formula (see Figure 4). However, from Table 1, the $Fe_3O_4$ nanoparticles size increases as the annealing temperature increases.

**Table 1** Effect of change in temperature toward the mean size of magnetite nanoparticles

| Sample | Annealing temperature (ºC) | Mean particles size (nm) |
|---|---|---|
| S1 | 200 | 2.02 |
| S2 | 300 | 5.58 |
| S3 | 400 | 8.35 |

### 2.3 Characterization

A sample was characterized using the Fourier Transform Infrared Spectrum (FTIR) (Perkin Elmer Spectrum 100 FTIR spectrometer). The absorption spectra of the magnetite nanoparticles were determined using Ultraviolet (Uv-Vis) spectroscopy (SHIMDZU 1800 UV-visible series). The X-ray diffraction spectroscopy (XRD) (Shimadzu XD-610) is used to determine the phase structure of the magnetite nanoparticles; the rays were radiated at a wavelength of ($\lambda$ = 0.15406 nm). However, the morphological analysis of the particles were obtained by Field Emission Scanning Electron Microscope (FESEM JEOL model JDM-7600F) equipped with X-ray dispersive spectrometer (EDS). To quantitatively examined the high and three dimension (3D) profiles of the structure formed by $Fe_3O_4$, Atomic Force Microscopes (AFM) (Bruker 59 × 413) was used in the tapping mode to image the topography of a two-layer grid formed by $Fe_3O_4$. The 3D image showed the spatial profiles of the grids.

## 3. RESULT AND DISCUSSION

### 3.1 Fourier Transform Infrared Spectra (FTIR) Analysis

The analysis of the infrared (IR) spectra confirms the monomer fixation of $Fe_3O_4$ nanoparticles (Figure 1), which resulted in the formation of Fe-O bands which is proven by the appearance of the absorptions band at 476cm$^{-1}$, 519cm$^{-1}$, 688cm$^{-1}$, 743cm$^{-1}$ and 875cm$^{-1}$ [7-10]. Moreover, the existence of peaks at 1069cm$^{-1}$ to 1600cm$^{-1}$ and 2606cm$^{-1}$ to 2941cm$^{-1}$ are assigned to O-H stretching, C-H stretching, C=C stretching, C=O stretching and C-O stretching bands respectively, indicating acidic medium condition of $Fe_3O_4$ nanoparticles preparation [19, 23]. The bonds appear at 3226cm$^{-1}$, 3293cm$^{-1}$ and 3325cm$^{-1}$ may be attributed to the $H_2O$ molecules or O-H vibrating stretching which are probably existed due to ethylene glycol $(CH_2OH)_2$ [24].

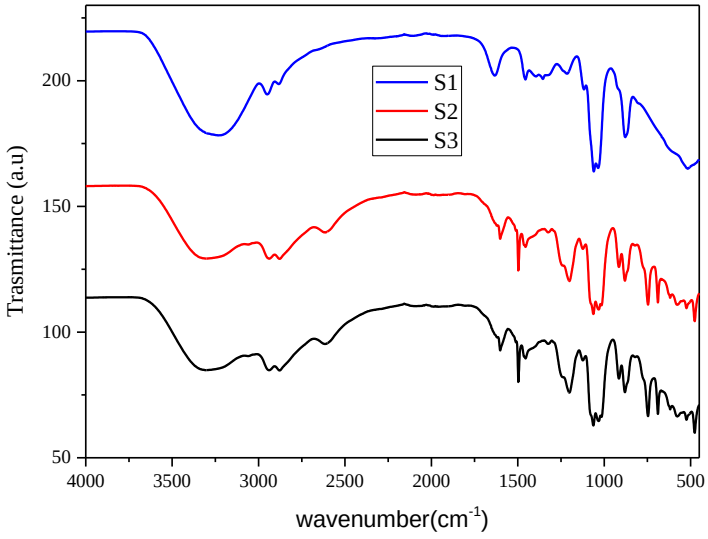


**Figure 1.** FTIR spectra of the magnetite nanoparticles.

### 3.2 UV-Visible Spectroscopy Study

The UV-visible spectroscopy was used to characterize the structure of $Fe_3O_4$ nanoparticles. Figure 2 reveals that the absorption peaks of the prepared $Fe_3O_4$ nanoparticles was found within the average UV-vis absorption region [5, 17], the average lower absorption wavelength of 262.13nm and 230 nm is observed in all the samples. This can easily be assigned to the intrinsic band gap absorption of the magnetite nanoparticles. The mobility of electrons from valence band to conduction band can be determined by the equation of the energy gap (Eg) of the $Fe_3O_4$ nanoparticles, was calculated using the relation

$$Eg = \frac{hc}{\lambda} \tag{1}$$

Where c is the velocity of light, h is the Planck constant, λ is the wavelength of light the estimated band gap energy result is 4.7.eV

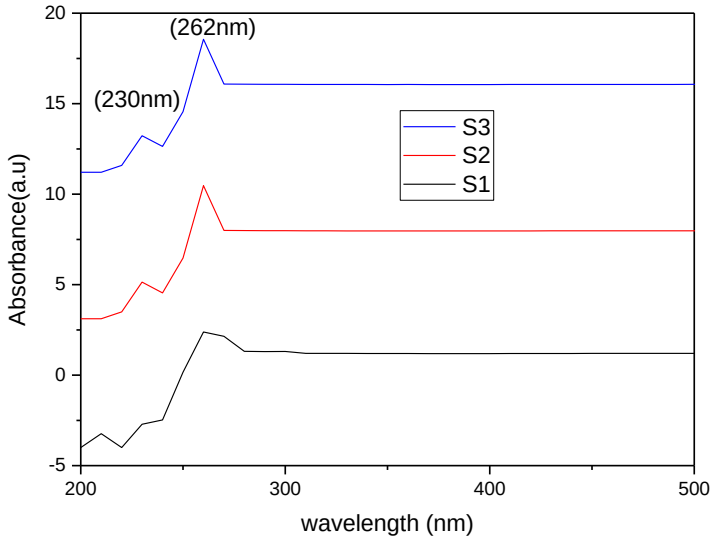


**Figure 2.** UV-visible spectra of the magnetite nanoparticles.

### 3.2 The Analysis Pattern of XRD in Magnetite ($Fe_3O_4$) Nanoparticles

The X-ray diffraction (XRD) pattern of the $Fe_3O_4$ nanoparticles was obtained at different annealing temperatures as shown at diffraction peak of 2θ = 26.75º, 32.67º, 35.44º, 55.88º, and 62.55º. This can be assigned to (310), (110), (311), (440), and (330) crystal planes of pure $Fe_3O_4$ nanoparticles with spinal structure of (JCPDS98-3969) [7, 21], respectively in 200ºC and 300ºC. At 400ºC some peaks are also observed at 46.54º and 55.98º which can be easily be assigned to (331), and (240). This indicates that these peaks are related to γ–$Fe_2O_3$ of (JCPDS98-0625) and α-$Fe_2O_3$ of (JCPDS98-2012) [22, 23] respectively, these data are in agreement with what was reported by [16, 18]. This reveals that the resultants nanoparticles in the first sample (S1) is purely $Fe_3O_4$ nanoparticles [25], while the remaining second (S2) and third (S3) samples are probably γ–$Fe_2O_3$ and α-$Fe_2O_3$ nanoparticles, respectively [26]. The peak of the sample S1 in Figure 3 matched very well with $Fe_3O_4$ of (JCPDS98-3969) nanoparticles, same peaks are shifted slightly to the higher angle in the S2, which is possibly due to oxidation of $Fe_3O_4$ in air at 300ºC resulted to γ–$Fe_2O_3$ same result of this transformation of $Fe_3O_4$ to γ–$Fe_2O_3$ have been reported in the literature by [13, 25] . The XRD pattern of the S3 indicates the oxidation of $Fe_3O_4$ at 400ºC in air. The diffraction peaks matched well with α-$Fe_2O_3$ (JCPDS98-2012), showing the transformation of $Fe_3O_4$ to α-$Fe_2O_3$ at 400ºC in air [8, 11].

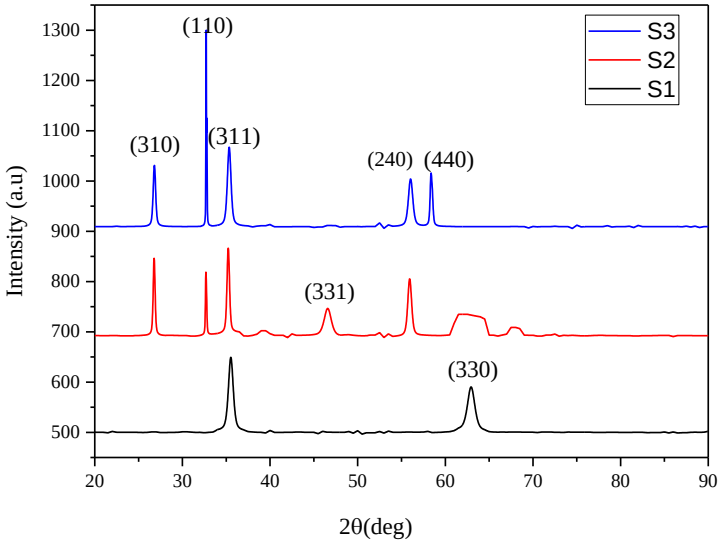


**Figure 3.** XRD analysis of $Fe_3O_4$ nanoparticles obtained at different temperature.

The following is the Scherer's formula used to calculated the crystalline particles size:

$$D = \frac{K \cdot \lambda}{\beta \cdot Cos\theta} \tag{2}$$

Where K (0.94) is a dimensionless quantity, λ is the X-ray wavelength, $\beta$ is the line broadening at half-maximum intensity (FWHM) and $\theta$ is the Bragg angle. Therefore, the obtained particles size result is plotted as the function of temperature in (Figure 5). As observed in the plot, the magnetite nanoparticles size increase as the temperature increases from 200ºC to 400ºC. Therefore, the average particles size as calculated by Scherer`s formula is 2.02nm, 5.58nm and 8.35nm for S1, S2, and S3 respectively. This shows that, with rising annealing temperatures, the size of the $Fe_3O_4$ nanoparticles is gradually increasing as shown.

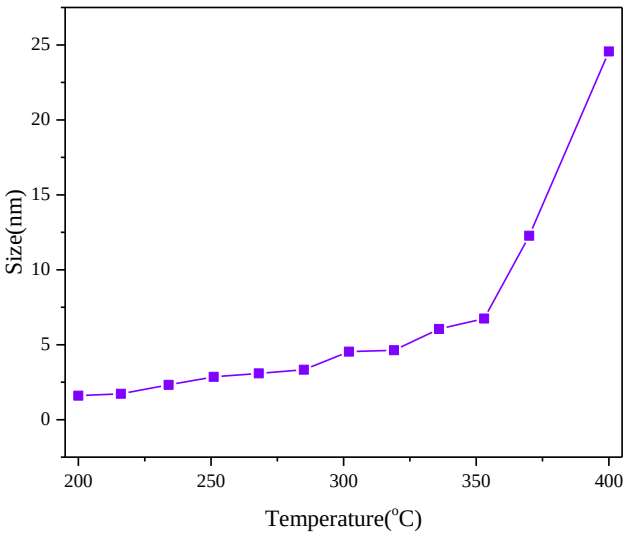


**Figure 4.** Size of $Fe_3O_4$ nanoparticles calculated using Scherer's formula as a function of annealing temperature.

### 3.3 Field Emission Scanning Electron Microscope (FESEM) and Energy Dispersive Spectrometer (EDS) Image of Magnetite ($Fe_3O_4$) Nanoparticles

FESEM observed the morphologies of the ($Fe_3O_4$) nanoparticles; the obtained images are shown in (Figure 5). The $Fe_3O_4$ nanoparticles sample (S3) annealed at 400ºC appeared in a spherical structure and nearly agglomerated. However, the spherical nanoparticles exhibit magnificent internationalisation rate and highest cellular take up instead of another shape such as nanorods, nanocubes or nanodisk [25]. Moreover, due to strong inter-particles Van der Waals force and magnetic attraction among the $Fe_3O_4$ nanoparticles, some agglomeration is detected in the samples (S3). The irregular shapes are observed at elevated changes in temperature (see S1 and S2) due to agglomeration process [22, 23]. The image obtained through EDS analysis shown in (Figure 5) confirmed the appearance of $Fe_3O_4$ nanoparticles by indicating Fe-O group of the element.

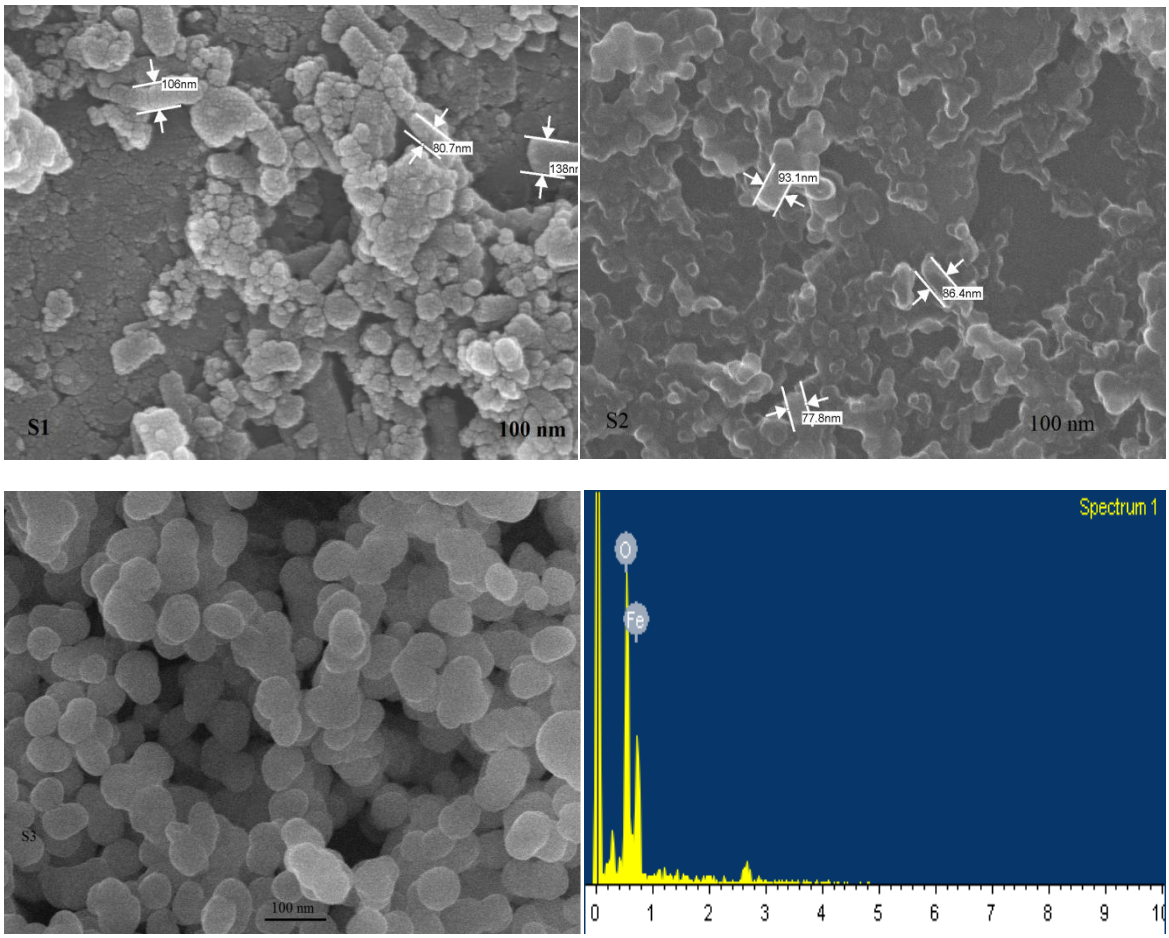


**Figure 5.** FESEM image of mag netite nanoparticles annealed under vacuum at 200 for S1, 300 for S2 and 400 $^0$C for S3 and the EDS image of magnetite ($Fe_3O_4$) nanoparticles.

### 3.4 Atomic Force Microscope (AFM) Characterization

The magnetite nanoparticles were deposited and dried on the glass for AFM characterization. The results were obtained to determine the three dimensions (3D) and roughness of the samples. Figure 5 shows the resulting 3D images of the sample, the maximum high of the particles is about 10.4nm and the diameter of 79.09nm for the scanned area of $1\mu m \times 1\,\mu m$ according to histogram in Figure 6. This results is in agreement with particles size obtained by FESEM. The knobs spots (yellow spots) indicate the present of small agglomeration of $Fe_3O_4$

nanoparticles, which is also seen as a yellow area at phase contrast of the 3D image as reported by [23]. The light yellow area is obtained due to the high moisture content in the ethylene glycol; the sample was melted down because of heat absorption from the laser light [26-28].

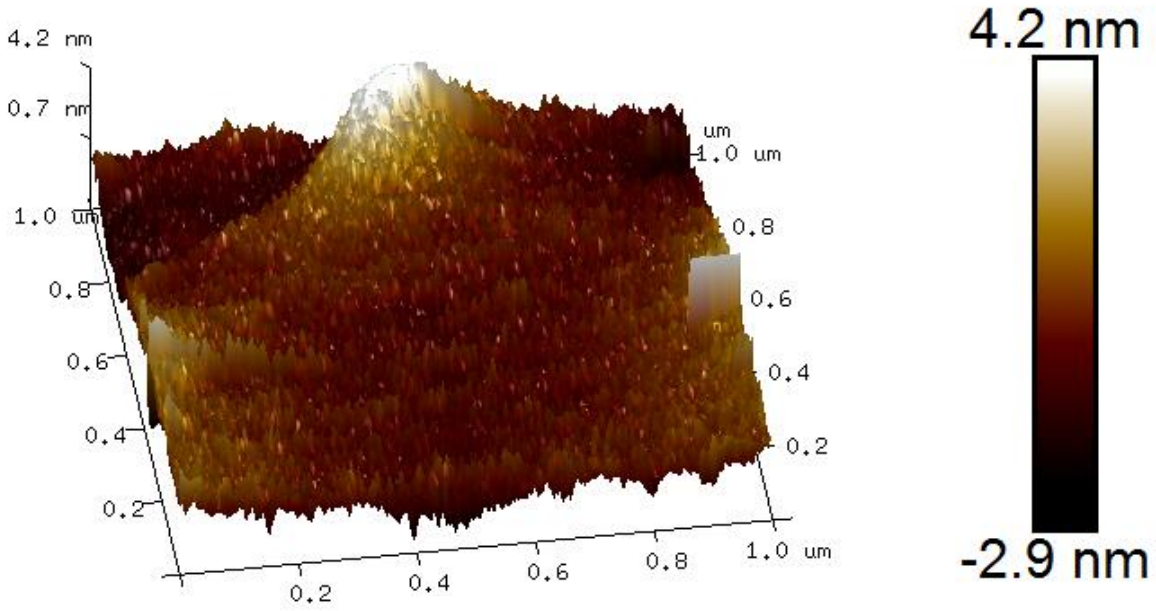


**Figure 5.** AFM 3D image of the magnetite nanoparticles annealed at 400ºC.

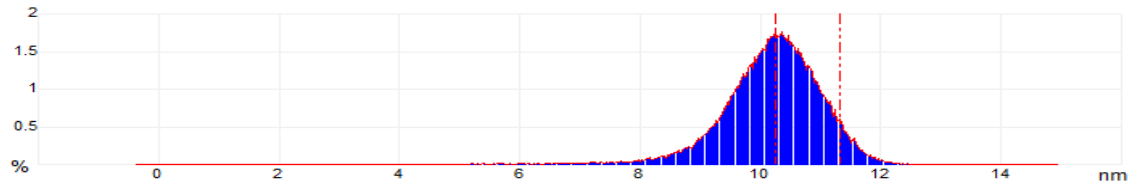


**Figure 6.** Histogram obtained from AFM Analysis.

## 4. CONCLUSION

This research has demonstrated the preparation of $Fe_3O_4$ nanoparticles by sol-gel assisted method and annealed under vacuum at different temperature 200-400ºC. The phase and molecular structure, functional group, morphologies and roughness analysis of the $Fe_3O_4$ nanoparticles were successfully characterized; the results indicated that the different sized $Fe_3O_4$ nanoparticles were obtained, simply by varying annealing temperature. The morphologies observed by FESEM shows that the sample S3 annealed at 400ºC is more spherical and different size $Fe_3O_4$ nanoparticles were observed in S1, and S2 annealed at 200 and 300ºC respectively. This method offers several significant properties for the preparation of $Fe_3O_4$ nanoparticles. Firstly, the synthetic method is economically important and environmentally friendly, because it includes cheaper and toxic free iron salts. Secondly, the size of the obtained $Fe_3O_4$ nanoparticles can be easily controlled by varying the annealing temperature.

**ACKNOWLEDGEMENT**

The authors gratefully acknowledge the Centre for Graduate Studies (CGS) Universiti Tun Hussein Onn Malaysia (UTHM) and Universiti Teknologi Mara (UiTM) for their kind support and encouragement through this research.

**REFERENCES**

[1] H. Kavas, M. Günay, A. Baykal, M. S. Toprak, H. Sozeri & B. Aktaş, "Negative Permittivity of Polyaniline-Fe3O4 Nanocomposite,"J. Inorg. Organomet. Polym. Mater., **23**, 2 (2013) 306–314.

[2] S. Chattopadhyay, O. P. Bajpai & D. K. Setua, "A Brief Overview on Ferrite (Fe3O4) Based Polymeric Nanocomposites: Recent Developments and Challenges," J. Res. Updat. Polym. Sci., **3**, 4 (2015) 184–204.

[3] O. M. Lemine, *et al.,* "Sol–gel synthesis of 8nm magnetite (Fe3O4) nanoparticles and their magnetic properties," Superlattices Microstruct., (2012).

[4] H. Cui, Y. Liu & W. Ren, "and low temperature sol – gel synthesis of nearly monodispersed iron oxide nanoparticles," Adv. Powder Technol., **24**, 1 (2013) 93–97.

[5] X. L. Wang, L. Wei, G. H. Tao & M. Q. Huang, "Synthesis and characterization of magnetic and luminescent Fe3O4/CdTe nanocomposites using aspartic acid as linker," Chinese Chem. Lett., **22**, 2 (2011) 233–236.

[6] B. Li, X. Weng, G. Wu, Y. Zhang, X. Lv & G. Gu, "Synthesis of $Fe_3O_4$/polypyrrole/polyaniline nanocomposites by in-situ method and their electromagnetic absorbing properties," J. Saudi Chem. Soc., **21**, 4 (2017) 466–472.

[7] A. H. M. Yusoff, M. N. Salimi, M. F. Jamlos & A. Yusoff, "Synthesis and characterization of biocompatible $Fe_3O_4$ nanoparticles at different pH Synthesis and Characterization of Biocompatible $Fe_3O_4$ Nanoparticles at Different pH," AIP Conf. Proc., **1835** (2017) 20010–20004.

[8] O. M. Lemine, *et al.,* "Sol–gel synthesis of 8nm magnetite (Fe3O4) nanoparticles and their magnetic properties," Superlattices Microstruct., **52**, 4 (2012) 793–799.

[9] M. Bhaumik, A. Maity & V. K. Gupta, "Synthesis and characterization of Fe 0 /TiO 2 nano-composites for ultrasound assisted enhanced catalytic degradation of reactive black 5 in aqueous solutions," J. Colloid Interface Sci., **506** (2017) 403–414.

[10] M. Aghazadeh & F. Aghazadeh, "Improve Synthesis of Iron Oxide Nanorode with Hydrothermal Method," **74** (2013) 67–74.

[11] J. B. Mamani, L. F. Gamarra & G. E. de S. Brito, "Synthesis and characterization of Fe3O4 nanoparticles with perspectives in biomedical applications," Mater. Res., (2014).

[12] X. Han & Y.-S. Wang, "Studies on the synthesis and microwave absorption properties of $Fe_3O_4$/polyaniline FGM," Phys. Scr., T**129** (2007) 335–339.

[13] J. Xu, *et al.,* "Preparation and magnetic properties of magnetite nanoparticles by sol-gel method," J. Magn. Magn. Mater., (2007).

[14] W. S. Chiu, S. Radiman, M. H. Abdullah, P. S. Khiew, N. M. Huang & R. Abd-Shukor, "One pot synthesis of monodisperse Fe3O4 nanocrystals by pyrolysis reaction of organometallic compound," Mater. Chem. Phys., **106**, 2–3 (2007) 231–235.

[15] J. B. Mamani, L. F. Gamarra & G. E. de S. Brito, "Synthesis and characterization of $Fe_3O_4$ nanoparticles with perspectives in biomedical applications," Mater. Res., **17**, 3 (2014) 542–549.

[16] Y. Yao, H. Jiang, J. Wu, D. Gu & L. Shen, "Synthesis of $Fe_3O_4$ /polyaniline nanocomposite in reversed micelle systems and its performance characteristics," Procedia Eng., **27** (2011) 664–670.

[17] N. J. Tang, W. Zhong, H. Y. Jiang, X. L. Wu, W. Liu & Y. W. Du, "Nanostructured magnetite ($Fe_3O_4$) thin films prepared by sol-gel method," J. Magn. Magn. Mater., **282**, 1–3 (2004) 92–95.

[18] Z. I. Taka, M. K. Mustafa, S. Asman, K. Ahmad, and S. Jibrin, "Preparation of Aniline Dimer-COOH Modified Magnetite ( $Fe_3O_4$) Nanoparticles by Ultrasonic Dispersion Method," vol. **7**, (2018) pp 185–188.

[19] Z. Jin, e*t al.,* "Enhanced magnetic and electrochemical properties of one-step synthesized PANI-Fe3O4 composite nanomaterial by a novel green solvothermal method," J. Alloys Compd., **695** (2017) 1807–1812.

[20] H. N. Azlina, J. N. Hasnidawani, H. Norita & S. N. Surip, "Synthesis of $SiO_2$ Nanostructures Using Sol-Gel Method," Acta Phys. Pol. A, **129**, 4 (2016) 842–844.

[21] S. Shafiee, O. Akhavan, H. Hatami & P. Hoseinkhani, "Sol-gel synthesis of thermoluminescent Cd-doped ZnTe nanoparticles," Indian J. Pure Appl. Phys., **53**, 12 (2015) 804–807.

[22] Z. I. Takai, M. K. Mustafa, and S. Asman, "Preparation of high performance conductive polyaniline magnetite (PANI/$Fe_3O_4$) Nanocomposites by Sol-Gel Method," *Asian J. Chem.*, vol. **30**, no. 12, (2018) 2625-2630.

[23] M. Bilton, S. J. Milne & A. P. Brown, "Comparison of Hydrothermal and Sol-Gel Synthesis of Nano-Particulate Hydroxyapatite by Characterisation at the Bulk and Particle Level," Open J. Inorg. Non-metallic Mater., **2**, 1 (2012) 1–10.

[24] M. Jamal, M. Z. Noh, S. Al-juboor, M. Haziman, B. Wan, and Z. Ibrahim, "Mechanical Properties of the Concrete Containing Porcelain Waste as Sand," vol. **7**, (2018) pp. 180–184.

[25] M. Jamshidiyan, A. S. Shirani & G. Alahyarizadeh, "Solvothermal synthesis and characterization of magnetic Fe3O4 nanoparticle by different sodium salt sources," Mater. Sci., **35**, 1 (2017) 50–57.

[26] S. Shaker, S. Zafarian, C. S. Chakra & K. V. Rao, "preparation and characterization of magnetite nanoparticles by sol-gel method for water treatment," Int. J. Innov. Res. Sci. Eng. Technol., **2**, 7 (2013).

[27] M. Niederberger, "Nonaqueous Sol – Gel Routes to Metal Oxide Nanoparticles," Acc. Chem. Res., **40**, 9 (2007) 793–800.

[28] J. Mohammed *et al.*, "Tuning the dielectric and optical properties of Pr–Co–substituted calcium copper titanate for electronics applications," *J. Phys. Chem. Solids*, vol. 126, no. September **201**(8)**,** pp. 85–92, 2019.